hep-ph/9508323
DPNU-95-20

Confinement and complex singularities in QED3

P. Maris*
Department of Physics, Nagoya University, Nagoya 464-01, Japan
(June 1995)

Abstract

The standard approximations of the Dyson–Schwinger equation lead to complex singularities of the fermion propagator. In three-dimensional QED one can show that this phenomenon might be related to confinement: a confining potential leads to mass-like singularities at complex momenta, and thus to the absence of a mass singularity on the real timelike axis. The correct treatment of the vacuum polarization is essential for the confining nature of QED3.

11.10.Kk,11.15.Pg,11.15.Tk,11.55.Bq

I. INTRODUCTION

Quarks are not observed as free particles, but only indirectly inside hadrons; this confinement of the quarks is an essential and very intriguing property of QCD, both from a theoretical and from an experimental point of view. Despite a lot of effort, there are still a lot of open questions about the confinement mechanism and confined particles. One of such questions is what the behavior of the full propagator of a confined particle is: e.g. does it have the same kind of analyticity properties as a bare quark propagator? If the full quark propagator has no mass singularity in the timelike region, it can never be on mass-shell and thus never be observed as a free particle [1,2,3,4]. So in this way the absence of a mass singularity implies directly confinement, and thus the analytic structure of the full quark propagator might be connected with confinement.

Since confinement is a nonperturbative phenomenon, the analytic properties of the full fermion propagator in a confining theory have to be studied in a nonperturbative way. The Dyson–Schwinger equation is a very powerful tool to study nonperturbative phenomena, and it is commonly used for studying dynamical chiral symmetry breaking, but it can also be useful in studies of confinement [5]. The usual truncation schemes of the Dyson–Schwinger equation show that the full fermion propagator in QED and QCD has complex branchpoints, instead of the expected mass singularity on the real timelike axis [6,7,8,9,10]. Although this phenomenon might be an artifact of the approximations, as believed about 15 years ago when it was first discovered [6], it has been suggested more recently that it might be a genuine property of the full theory, connected with confinement, especially in QCD [7,8,9]. If the quark propagator has a mass-like singularity at complex momenta, instead of a mass singularity in the timelike region, it can never be on mass-shell and is thus confined.

Not only in QCD the fermions are confined, also in several other theories there is confinement. Quantum electrodynamics in two space- plus one time-dimension (QED3) is such a theory, with a confining potential for the fermions, at least at the classical level; for the full theory it depends on the behavior of the vacuum polarization [11]. It is also a very interesting model to study dynamical mas generations, and for this purpose the Dyson–Schwinger equation has been extensively studied on the Euclidean axis [12,13,14,15,16,17]. The theory is super-renormalizable, and does not suffer from the ultraviolet divergences which are present in the corresponding four-dimensional theories. That means that we do not need to introduce any artificial cutoff, and the only mass scale in massless QED3 is the dimensionful coupling. In this way we are provided with a very interesting model, from which we can learn a lot about the analytic structure of the propagator, and which is mathematically easier to analyze than four-dimensional theories. The result can be very useful as guidance for other, more complicated, theories like QCD. Apart from the the interesting features connected with dynamical mass generation and confinement in general, it might also have some direct physical relevance, both in condensed matter physics (in connection with phenomena occurring in planes) and as the high-temperature limit of the corresponding four-dimensional theory.

In this paper we study the analytic structure of the fermion propagator in QED3, using the Dyson–Schwinger equation and some different approximations for the full photon propagator. We show that, if there is a confining potential, the fermion propagator has complex mass-like singularities, but if there is no confining potential, the mass singularities

are located almost on the real timelike axis, as we would expect. The presence or absence of the confining potential depends on the particular approximation for the photon propagator.

This paper is organized as follows: in the next section we review the analytic structure of the fermion propagator in the context of perturbation theory and what we would expect for the propagator of a confined particle. In Sec. III we introduce the model we are considering and its confining properties. Next, we discuss the Dyson–Schwinger equation, the truncation scheme we are using, and our numerical procedures. In Sec. V we present our results, and finally we give some conclusions in Sec. VI.

II. ANALYTIC STRUCTURE OF PROPAGATORS

A. Mass singularities

The analytic structure of the bare fermion propagator is well-known: in momentum space, it has a single pole at the bare mass of the fermion. In Minkowski metric (which we will use in this section only, out of convenience), we have for the bare propagator

$$S(p) = \frac{1}{\not{p} - m_0 + i\varepsilon}\,, \tag{1}$$

with a mass-pole which is located at timelike momentum $p^2_{\text{Mink}} = m_0^2$. The integration contour one encounters in all kinds of calculations, goes around this singularity due to the $i\varepsilon$-prescription, and this $i\varepsilon$ also allows us to perform the usual Wick rotation from Minkowski space to Euclidean space.

In perturbation theory, the full fermion propagator has a similar structure, at least on the first Riemann sheet: a single pole at the physical mass of the particle, and a more complicated structure for momenta beyond some threshold energy for multi-particle production, see Fig. 1. If we are dealing with massless particles, as in QED, where we have massless photons, this single pole becomes a logarithmic branchpoint, see e.g. [18].

In general, we expect a similar structure for the full fermion propagator in a nonperturbative calculation, at least if the fermion corresponds to a stable physical particle. In a theory of interacting particles *with asymptotic states* we have the Källen–Lehmann representation

$$S_F(p) = Z_2 \frac{\not{p} + m_{\text{phys}}}{p^2 - m^2_{\text{phys}}} + \int_{\tilde{m}^2}^{\infty} \mathrm{d}\mu^2 \frac{\not{p}\rho_1(\mu^2) + \rho_2(\mu^2)}{p^2 - \mu^2 + i\varepsilon}\,, \tag{2}$$

with the spectral weight functions $\rho_i(p^2)$ real and nonnegative, and $\tilde{m} \geq m_{\text{phys}}$ the threshold for multi-particle production. We therefore expect a full electron propagator with a mass singularity at the physical mass of the electron, which is located on the real axis in the timelike region at $p^2_{\text{Mink}} = m^2_{\text{phys}}$, and a logarithmic branch-cut along the real axis, beyond this singularity.

However, the derivation of the Källen–Lehmann representation breaks down in the absence of the asymptotic states; the above argument only holds in cases were the fermion is indeed a stable, physically observable particle. If we are considering a theory with confined fermions, which means that there are no asymptotic states for these fermions, we do not

have a rigorous proof of the existence of a Källen–Lehmann representation, so we do not know a priori the analytic structure of the propagator of such a confined particle.

The mass singularities of the propagator at the physical mass of the particle are crucial for the existence of observable asymptotic states. Without such mass singularities, the particles can never be on mass shell, and thus never be observed as real particles. In other words, confinement might very well be related to the absence of such mass singularities, and thus to the absence of a Källen–Lehmann representation for the propagator of such a particle [1,2,3,4].

B. Complex singularities

If the propagator of a confined particle does not have a a Källen–Lehmann representation, what (other) analytic structure can we expect? Writing the full fermion propagator as

$$S(p) = Z(p^2)\frac{\not{p} + m(p^2)}{p^2 - m^2(p^2)}\,, \tag{3}$$

we can now ask the question: what analytic structure is possible? In principle there are the following possibilities:

- the propagator has complex singularities (at zeros of the denominator);
- the propagator is an entire function;
- the propagator has compensating zeros (both the denominator and the wavefunction renormalization $Z(p)$ are zero at the same point, which might be located in the timelike region).

During the last couple of years, analyses of the fermion propagator using the Dyson–Schwinger equation in the complex momentum plane show complex mass-like singularities in a variety of models and truncation scheme. This phenomenon was first discovered by Atkinson and Blatt [6] in quenched ladder QED4, and it was generally believed to be an artifact of the approximations. However, in a theory with confined particles, it might very well be a genuine property of the full theory: the absence of a mass singularity at timelike momenta will effectively confining the particles, in the sense that they will not be observable as physical stable states. Recently, it has been suggested by several authors, that the complex singularities one finds by solving the Dyson–Schwinger equation for complex momenta, are indeed a signal for confinement, especially in a confining theory like QCD [7,8,9]. In this paper we show that there is indeed a connection between a confining potential and complex mass-like singularities in QED3.

Note however that also other analytic structures, like a fermion propagator which is an entire function, will effectively confine the fermions; and in principle there are also other confinement mechanisms possible which do allow for a physical mass pole for the fermion propagator.

III. QED3

A. Formalism

In Minkowski space, we need the artificial $i\varepsilon$ description, in order to define the path integrals, and to select the integration path around the mass singularities in all kinds of calculations. Alternatively, we could set up our field theory in Euclidean space, in which case the integrals are well-defined from the beginning. In principle the Wick rotation allows us to go from Euclidean to Minkowski space and back, and both formulations seem to be equivalent, but in the presence of complex singularities this easy connection between Euclidean and Minkowski space is destroyed. Since the theory is better defined in Euclidean metric, we will use that formalism. Once we know the Euclidean Green's functions, we can obtain the Wightman functions in coordinate space by an analytic continuation in the time-coordinates, and from them the physically relevant Minkowski Green's functions [19]. In this way we can (in principle) extract all of the physically relevant information in Minkowski space, even after setting up the formalism in Euclidean space.

The Lagrangian in Euclidean space is

$$\mathcal{L}(\psi,\bar{\psi},A) = \bar{\psi}\left(\gamma^\mu(\partial^\mu + ieA^\mu) + m_0\right)\psi + \tfrac{1}{4}F^{\mu\nu}F^{\mu\nu} + \tfrac{1}{2a}(\partial^\mu A^\mu)^2\,. \tag{4}$$

In QED3, only three anti-commuting γ-matrices are needed, which can be realized by taking a two-dimensional representation for these matrices, e.g. the Pauli spin matrices. In that case we also have two-dimensional spinors, instead of the four-dimensional spinors one would use in four-dimensional theories. However, here we will use the formulation with a four-dimensional spinor-space, and use the same γ-matrices as in four space-time dimensions. In order to study dynamical mass generations, and its influence on confinement, we take the bare fermions to be massless: $m_0 = 0$. In QED3 with four-dimensional spinors one can have two types of mass terms for the fermions, namely a parity-breaking and a parity-conserving mass term. We will only consider the dynamical generation of a parity-even mass [13]; it has been shown that there is no dynamical breakdown of parity [20].

The full fermion propagator can be written as

$$S^{-1}(p) = Z(p)\left(i\not{p} + m(p)\right)\,, \tag{5}$$

and the full photon propagator is

$$D^{\mu\nu}(q) = \frac{1}{q^2(1+\Pi(q))}\left(\delta^{\mu\nu} - \frac{q^\mu q^\nu}{q^2}\right) + a\frac{q^\mu q^\nu}{q^4}\,, \tag{6}$$

in a general covariant gauge. In this equation, $\Pi(q)$ is the vacuum polarization, a the gauge parameter, $m(p)$ the dynamical mass function of the fermion, and $Z(p)$ the fermion wavefunction renormalization. For sake of simplicity, we use the Landau gauge ($a = 0$).

The exact Dyson–Schwinger equation for the fermion propagator is

$$S^{-1}(p) = i\not{p} + e^2\int\frac{\mathrm{d}^3k}{(2\pi)^3}\gamma^\mu S(p)\Gamma^\nu(p,k)D^{\mu\nu}(p-k)\,, \tag{7}$$

with the unknown full vertex $\Gamma^\nu(p,k)$, and the full photon propagator $D_{\mu\nu}(p-k)$. In analyzing the fermion Dyson–Schwinger equation, we have to truncate this equation. In this paper, we discuss both the socalled quenched ladder approximation (bare photon and bare vertex), and two approximations based on the $1/N$ expansion.

B. $1/N$ Expansion

A very popular truncation scheme in QED3 is the $1/N$ expansion: consider N massless fermion flavors, and use the large N limit in the following way: let $N \to \infty$ and $e^2 \to 0$ in such a way that the product $e^2 N$ remains fixed. It has been shown that massless QED3 is infrared finite order by order in such a $1/N$ expansion [21]. For convenience we choose the coupling, which defines our mass scale, to be

$$e^2 = \frac{8\alpha}{N}\,, \tag{8}$$

and keep α fixed.

Such a $1/N$ expansion means that we have to take into account the one-loop vacuum polarization: the coupling is of order $1/N$, but there are N fermion loops contributing to the vacuum polarization tensor

$$\Pi^{\mu\nu}(q) = -e^2\, N \int \frac{\mathrm{d}^3k}{(2\pi)^3} \mathrm{Tr}\left[\gamma^\mu S(k+q)\Gamma^\nu(k+q,k)S(k)\right]\,. \tag{9}$$

This vacuum polarization tensor has an ultraviolet divergence in its part proportional to $\delta^{\mu\nu}$, which can be removed by evaluating it using a gauge-invariant regularization scheme. Defining the vacuum polarization $\Pi(q)$ by

$$\Pi^{\mu\nu}(q) = \left(q^2\delta^{\mu\nu} - q^\mu q^\nu\right)\Pi(q)\,, \tag{10}$$

we can get the regularized vacuum polarization by contracting the vacuum polarization tensor with [5,11]

$$\left(q^2\delta^{\mu\nu} - 3q^\mu q^\nu\right)/q^4\,, \tag{11}$$

which is orthogonal to $\delta^{\mu\nu}$ and thus projects out the divergent part. Note that this regularization gives the same result as dimensional regularization, but this projection is much easier to perform if we take into account dynamical fermions, in Sec. V C. Using bare, massless fermions and a bare vertex, we have for this vacuum polarization

$$\Pi(q) = \frac{e^2\, N}{8\sqrt{q^2}} \;=\; \frac{\alpha}{q}\,, \tag{12}$$

whereas the one-loop vacuum polarization with massive fermions gives

$$\Pi(q) = \frac{2\alpha}{\pi\, q^2}\left(2m + \frac{q^2-4m^2}{q}\arcsin\frac{q}{\sqrt{q^2+4m^2}}\right)\,. \tag{13}$$

The crucial difference between the vacuum polarization with massless and with massive fermions lies in the infrared region: with massless fermions the vacuum polarization blows up at the origin, $\Pi(0) \to \infty$. With massive fermions however, with a constant mass m, the vacuum polarization is finite in the infrared

$$\Pi(0) \to \frac{4\alpha}{3\pi\, m}\,. \tag{14}$$

C. Confining potential

One of the interesting properties of QED3 is that it exhibits confinement [22]. We can define a "classical" potential for the fermions in coordinate space [11]

$$V(\vec{x}) = -e^2 \int \frac{\mathrm{d}^2 q}{(2\pi)^2} e^{i\vec{q}\cdot\vec{x}} \frac{1}{\vec{q}^2(1+\Pi(\vec{q}^2))}\,, \tag{15}$$

where $\Pi(q)$ is the vacuum polarization. In lowest order in perturbation theory, we can neglect the effects of the vacuum polarization and simply calculate the potential. This leads to a logarithmically rising potential

$$V(\vec{x}) = \frac{e^2}{2\pi} \ln(e^2|x|)\,. \tag{16}$$

Because this potential increases at large distances, it effectively confines the fermions, and there are no free asymptotic one-fermion states possible.

Of course, this potential will change under the influence of the vacuum polarization. As our results show, the correct inclusion of the vacuum polarization is indeed essential for confinement. The relevant region for the question whether or not there is a confining potential is the infrared region, corresponding to large spatial separations in configuration space. As is shown by Burden *et al.* [11], under quite general and natural conditions for the vacuum polarization, the potential associated with the full photon propagator behaves like

$$V(\vec{x}) = \frac{e^2 \,\ln\left(e^2|x|\right)}{\left(1+\Pi(0)\right)2\pi} + \text{constant} + \mathcal{O}\left(\frac{1}{|x|}\right)\,. \tag{17}$$

This behavior can be derived assuming that the vacuum polarization is bounded and continuously differentiable for Euclidean momenta, and that it falls of at least as $1/q$ as $q \to \infty$.

From this equation, we can see immediately that, depending on the behavior of the vacuum polarization in the infrared region, there are two possibilities

- a confining potential if $\Pi(0)$ is finite;
- no confining potential if $\Pi(0) \to \infty$.

If we know look at the one-loop perturbative vacuum polarization, we see that there is an essential difference between massless and massive QED3. For massive fermions, the vacuum polarization at the origin, $\Pi(0)$, is finite as can be seen from Eq. (14). Therefore there is a logarithmically confining potential in leading order in $1/N$ for massive fermions.

On the other hand, if the fermions are massless, there is no confining potential to leading order to $1/N$; the one-loop vacuum polarization blows up at $q^2 \downarrow 0$, see Eq. (12), and the photon propagator is softened in the infrared region. Perturbatively, to leading order in $1/N$, the fermion propagator is just the bare propagator, with a single pole at the origin, corresponding to an observable massless fermion. However, a dynamically generated fermion mass might very well change this leading-order behavior.

IV. DYSON–SCHWINGER EQUATION

In order to determine the analytic structure of the fermion propagator nonperturbatively, we use the Dyson–Schwinger equation. In general, after reducing the γ-algebra, the Dyson–Schwinger equation, Eq. (7), becomes

$$Z^{-1}(p)\, m(p) = e^2 \int \frac{\mathrm{d}^3k}{(2\pi)^3} \tfrac{1}{4} \mathrm{Tr}[\gamma^\mu S(k) \Gamma^\nu(p,k) D^{\mu\nu}(q)]\,, \tag{18}$$

$$Z^{-1}(p) = 1 - \frac{e^2}{p^2} \int \frac{\mathrm{d}^3k}{(2\pi)^3} \tfrac{1}{4} \mathrm{Tr}[\not{p}\gamma^\mu S(k) \Gamma^\nu(p,k) D^{\mu\nu}(q)]\,, \tag{19}$$

with the photon propagator $D^{\mu\nu}(q)$ as defined by Eq. (6), with the unknown vacuum polarization, and the unknown full vertex function $\Gamma^\nu(p,k)$. The general approach to solve this equation is to choose a specific truncation scheme for the vertex and the photon propagator, and then to solve the resulting equations numerically.

A. Truncation scheme

Here, we will adopt the bare vertex approximation, replacing the full vertex by the bare one, γ^μ. We also neglect the effects of the wavefunction renormalization, so we put $Z(p) = 1$. This truncation is based on the leading-order behavior of the vertex and the wavefunction renormalization in the $1/N$ expansion. Such an approximation scheme is also consistent with the requirement following from the Ward–Takahashi identity that the wavefunction renormalization and the vertex renormalization are equal. It is usually referred to as the ladder or rainbow approximation, and it leads to a finite critical number of fermion flavors below which the chiral symmetry is broken dynamically [1]. Note that in the Landau gauge, with a bare photon propagator and bare vertex (the quenched ladder approximation), Eq. (19) gives $Z(p) = 1$ exactly.

For the photon propagator we use some different approximations, to determine the influence of the infrared behavior of the vacuum polarization on the analytic structure of the fermion propagator and on the (confining) potential. We compare in detail the results as obtained in

1. the quenched approximation: a bare photon propagator;
2. the $1/N$ expansion using the analytical formula for the one-loop vacuum polarization with bare, massless fermions, Eq. (12)
3. the $1/N$ expansion using the one-loop vacuum polarization with full fermions, *with the dynamically generated fermion mass function.*

---

[1] Using this approximation, the equation for the wavefunction renormalization, Eq. (19), is formally satisfied up to order $1/N$. It is known that the effects of the wavefunction renormalization (together with a more sophisticated Ansatz for the vertex) will change the results found in this $1/N$ truncation scheme [15,16,17], but we will not address that problem here.

In both 2 and 3, we take a bare vertex in the expression for the vacuum polarization.

This truncation scheme gives us the following expression for the mass function

$$m(p) = \frac{e^2}{2\,\pi^2} \int_0^\infty \mathrm{d}k \frac{k^2\, m(k)}{k^2 + m^2(k)} \mathrm{K}(p,k)\,, \tag{20}$$

$$\mathrm{K}(p,k) = \int_0^\pi \frac{\sin\theta\,\mathrm{d}\theta}{(p^2 - 2pk\cos\theta + k^2)(1 + \Pi(p^2 - 2pk\cos\theta + k^2))}\,, \tag{21}$$

with the kernel $\mathrm{K}(p,k)$ depending on the particular approximation we use for the photon propagator.

B. Numerical calculations

Once we have truncated the equations, we can solve the resulting integral equation for the mass function numerically. We start by solving the equation for Euclidean momenta $0 \leq p^2 < \infty$. However, we are not really interested in the result on the Euclidean axis (for a more detailed discussion about the existence of a critical number of fermion flavors for dynamical chiral symmetry breaking we refer to the literature [13,14,15,16,17]), but we want to know the behavior of the propagator in the complex momentum plane. For that purpose we have used two different approaches: one is a direct analytic continuation of the integral equation, Eq. (20), into the complex plane. This can be done by deforming the integration contour and solving the integral equation along this new contour. Note that it is not possible to keep the integration variable k real, and take only the external variable p complex (after solving the integral equation on the real axis), because of the analytic structure of the kernel $\mathrm{K}(p,k)$. With massless photons, and thus a photon propagator which has a singularity at the origin, there is a pinch singularity at $p = k$, and we are forced to integrate through the point $p = k$. So for complex momenta p we have to solve the integral equation along a deformed contour in the complex plane.

In practice, we change the integration contour by rotating it in the complex plane, multiplying both the internal and the external variable by a phase factor $\mathrm{e}^{i\phi}$, so we get the complex variables $\tilde{k} = \mathrm{e}^{i\phi}k$ and $\tilde{p} = \mathrm{e}^{i\phi}p$, see Fig. 2. Since in QED3 the integral falls off rapidly enough in the ultraviolet, there is no need to take into account the contribution coming from the arc at infinity, in contrast to theories with a finite cutoff like QED4. This procedure works quite well, until one comes close to a singularity caused by a zero of the denominator of the integration kernel

$$\frac{1}{k^2 + m^2(k)}\,, \tag{22}$$

where the numerical integration procedure becomes unstable. The location in the complex plane of the actual singularity itself can be obtained by extrapolating the numerical results to the "physical" mass μ, defined by the zero of this denominator

$$-\mu^2 + m^2(\sqrt{-\mu^2}) = 0\,. \tag{23}$$

For more details about our numerical procedure and the analytic continuation, we refer to [23]. In this way we can in principle find the singularities in the complex plane, but it is a very time-consuming numerical process, and does not always converge to a stable solution.

Therefore we also used another method, based on the Euclidean-time Schwinger function, to determine whether or not the propagator corresponds to a physical observable state [5,24]. We define

$$\sigma(p^2) = \frac{m(p)}{p^2 + m^2(p)}\,, \tag{24}$$

$$\Delta(t) = \int \mathrm{d}^2x \int \frac{\mathrm{d}^3p}{(2\pi)^3} \mathrm{e}^{i(p_3 t + \vec{p}\cdot\vec{x})} \sigma(p^2)\,. \tag{25}$$

Using this Schwinger function, one can show that if there is a stable asymptotic state associated with this propagator, with a mass m, then

$$\Delta(t) \sim \mathrm{e}^{-mt} \tag{26}$$

for large (Euclidean) t, so for the logarithmic derivative we get

$$\lim_{t\to\infty} \frac{\mathrm{d}}{\mathrm{dt}} \ln\left(\Delta(t)\right) = -m\,, \tag{27}$$

whereas two complex conjugate mass-like singularities, with complex masses $\mu = a \pm i\,b$, lead to an oscillating behavior like

$$\Delta(t) \sim \mathrm{e}^{-at} \cos\left(bt + \delta\right) \tag{28}$$

for large t. This method is much less time-consuming to see whether or not the propagator has a real mass-singularity or not, but it is less accurate than solving the Dyson–Schwinger equation for complex momenta in determining the (complex) mass-singularities.

V. RESULTS

A. Quenched QED3

In massless quenched QED3, there is no free parameter: the coupling in QED3 is dimensionful and thus defines the energy scale, and there are no other parameters. By choosing the Landau gauge, we satisfy the requirement that the wavefunction renormalization and the vertex renormalization are exactly equal: from Eq. (19) it follows directly that in quenched QED using the Landau gauge, $Z(p) = 1$, and the equation for the mass function reduces to

$$m(p) = \frac{e^2}{2\pi^2} \int_0^\infty \mathrm{d}k \frac{m(k)}{k^2 + m^2(k)} \frac{k}{2p} \ln \frac{(p+k)^2}{(p-k)^2}\,. \tag{29}$$

Solving this equation on the Euclidean axis shows that there is dynamical mass generation in this case, and the infrared mass $m(0)$ is proportional to the dimensionful coupling, as expected.

Next, we have calculated the Schwinger function, using the mass function on the Euclidean axis, see Fig. 3. This figure clearly shows that there is no stable asymptotic one-fermion state associated with this propagator, in other words, the fermions cannot be observed as free particles and are thus confined. The oscillations in this figure strongly suggest that the fermion propagator has complex mass-like singularities, corresponding to two complex-conjugate masses. Using

$$\Delta(t) \sim \mathrm{e}^{-at} \cos\left(bt + \delta\right), \tag{30}$$

to extract such a complex mass, we estimate this to be

$$\mu = (0.80 \pm 0.71\, i)\, m(0) \tag{31}$$

However, this method might be not very accurate in determining the actual value of the (complex) masses, since Eq. (30) only holds for large values of t, whereas for large values of t the numerical noise in calculating the Euclidean-time Schwinger function destroys the signal. So we have used values of t up to $t \sim 10/m(0)$ (we rescale all dimensionful quantities by $m(0)$), and use only the first oscillations to determine the imaginary part of the complex mass. Furthermore, Eq. (30) is based on the assumption that only these (complex) singularities contribute to the Schwinger function (at least at large t), but if there are complex singularities, there might be more than just two complex-conjugate mass-like singularities.

Therefore we also used the other method to determine the analytic structure of the propagator, and have solved the integral equation in the complex plane. This leads to two complex-conjugate singularities, located at

$$|\mu| = 0.104\, e^2 \;=\; 1.01\, m(0)\,, \tag{32}$$

$$\theta_\mu = \tfrac{\pi}{2} - \phi \;=\; 0.819\,. \tag{33}$$

This result confirms the estimate based on the Schwinger function, given the inaccuracy of the estimate of the complex mass.

So both the Schwinger function and a direct search for mass-like singularities show that there is a complex mass singularity, which makes it impossible for the fermion propagator to become on mass-shell, end thus effectively confines the fermion. This is in agreement with the fact that in quenched massless QED3 there is a confining potential.

B. One-loop vacuum polarization

Next, we include the one-loop vacuum polarization, using bare massless fermions, Eq. (12). As already mentioned before, perturbatively the $1/N$ expansion gives to leading order no confining potential, and a full fermion propagator which is the same as the bare one, and thus corresponding to a massless stable asymptotic state. In the case of dynamical mass generation, which we consider here, the situation is more complicated. Since the number of fermion flavors is the only free parameter in this case, we present our results as a function of N.

For simplicity we use Landau gauge, as in the quenched approximation, and we can perform the angular integration in the Dyson–Schwinger equation analytically to arrive at the equation for the mass function

$$m(p) = \frac{4\,\alpha}{N\,\pi^2} \int_0^\infty \mathrm{d}k \frac{m(k)}{k^2 + m^2(k)} \frac{k}{p} \ln \frac{|p+k| + \alpha}{|p-k| + \alpha}\,, \tag{34}$$

This can be solved numerically as an integral equation, or after expanding the logarithm and some further approximations reduced to a second-order nonlinear differential equation

[13]. Both the integral and the differential equation show that there is dynamical mass generation if $N < N_c = 3.24$, see Fig. 5; this critical number is in agreement with analytical calculations using bifurcation theory, leading to $N_c = 32/\pi^2$.

We have calculated the Schwinger function, using the mass function on the Euclidean axis, see Fig. 3. This figure strongly suggest that there is a stable asymptotic one-fermion state, which means that the fermions are not confined and can be observed. Up to the largest values of t at which the Schwinger function gives a numerically stable result, we find an almost constant logarithmic derivative. From this Schwinger function we have derived a value for the asymptotic mass for some different number of fermion flavors, and the results are listed in Table I. We do not find any evidence for oscillations which would signal a complex mass, as there were in the quenched approximation.

We have also solved the integral equation in the complex plane. This reveals that the mass singularities are not exactly on the real timelike axis, but that they do have small imaginary parts, see Table I. In Fig. 6 we have plotted the phase of these singularities as a function of N, by numerically solving both the integral equation and the differential equation which can be derived from Eq. (34), and those results almost coincide. Given the fact that we have only solved the truncated Dyson–Schwinger equation, it is not unreasonable to expect a small deviation of the physical mass from the real axis, and given the relative smallness of the imaginary part this could very well be an artifact of the approximations, especially since the singularity tends to move toward the real timelike axis if the number of flavors goes to the critical number.

The reason for not finding this imaginary part of the mass singularities using the Schwinger function lies in its smallness: since the imaginary part is of the order of 10% of the real part (or even less), we will not find a clear signal for it at $t \leq 10/m$, where m is the typical infrared mass-scale; however, the numerical noise destroys the signal completely at these (or larger) values of t.

So our conclusion is that this approximation, using the one-loop vacuum polarization of bare massless fermions, leads to (almost) stable observable asymptotic states, with an (almost) real physical mass. This agrees well with the fact that in this case we do not have a confining potential.

C. Full vacuum polarization

Finally, we include the one-loop vacuum polarization, Eq. (9), with dynamical fermions and a bare vertex. In other words, we consider the coupled Dyson–Schwinger equations for the photon and propagator, in the bare vertex approximation. This leads to two coupled integral equations to solve

$$m(p) = \frac{4\,\alpha}{N\,\pi^2} \int_0^\infty \mathrm{d}k \frac{k^2\,m(k)}{k^2 + m^2(k)} \int_{-1}^1 \frac{\mathrm{d}z}{(p^2 - 2pkz + k^2)(1 + \Pi(p^2 - 2pkz + k^2))}\,, \tag{35}$$

$$\Pi(q^2) = \frac{8\alpha}{q^2} \int \frac{\mathrm{d}^3k}{(2\pi)^3} \frac{2k^2 - 4k\cdot q - 6(k\cdot q)/q^2}{(k^2 + m^2(k))((k+q)^2 + m^2(k+q))}\,. \tag{36}$$

Again, this can be solved numerically: we start by solving the mass equation for a given vacuum polarization, and use that resulting mass function to calculate the vacuum polarization

numerically and iterate this procedure. Just as in the previous case, it leads to dynamical mass generation if the number of fermion flavors is below a critical number, see Fig. 5. The behavior of the infrared mass is quite similar, and also the critical number is the same as in the previous approximation, $N_c = 3.24$, as could be expected on grounds of bifurcation theory.

Also in this case we have calculated the Schwinger function, see Fig. 4. This shows that there are no stable asymptotic one-fermion states associated with this propagator, just as in quenched QED3, but in sharp contrast to the previous case. We have also shown the result with a fixed mass ($m = m(0)$) in the analytical formula for the vacuum polarization, Eq. (13). This gives qualitatively the same result as when using the dynamical mass function. In both cases the oscillations indicate complex mass-like singularities, and we have given estimates for these complex masses in Table I.

We have also solved the integral equation in the complex plane, which confirms the observation based on the Schwinger function that there are complex mass-like singularities. The phase of these singularities is plotted in Fig. 6, and for some different values of N we have given our result in Table I. Given the inaccuracy in the estimates based on the Schwinger function, there is a good agreement between both methods.

It is clear that the the effects of the fermion mass in the loop for the vacuum polarization confines the fermions: the potential becomes confining, the mass singularities move into the complex plane, and there are no stable observable asymptotic states.

D. Discussion of the results

Our results show that the correct treatment of the vacuum polarization is essential in a nonperturbative calculation of the fermion propagator. Based on bifurcation theory, one can argue that the influence of the dynamically generated mass function can be neglected in studying the chiral phase transition. Although this is indeed true for the value of the critical coupling, and maybe also for the behavior of the infrared mass $m(0)$ close to the critical coupling, it is certainly not true for the behavior of the *physical* mass, defined at the zero of $p^2 + m^2(p)$.

On the real axis, the dynamical mass function in quenched QED3 is qualitatively quite similar to the mass function in the $1/N$ expansion, both with massless fermions and with massive fermions in the vacuum polarization, see Fig. 7(a). There is a scale difference between the different approximations, but all mass functions are almost constant in the (far) infrared region, and fall of to zero as $1/p^2$ in the (far) ultraviolet. Only in the intermediate-energy region there are some differences due to the inclusion of the vacuum polarization.

In contrast, in the complex plane the behavior is not similar at all, leading to a drastic different analytic structure. This difference can be traced back to the difference in the infrared behavior of the photon propagator: with a confining photon propagator there are complex mass-like singularities, whereas with a deconfining photon propagator these singularities are located almost on the real timelike axis. Surprisingly, this difference can be seen very clearly by using the Euclidean-time Schwinger function, which can be calculated using the mass function on the real Euclidean axis only. So although the behavior of the mass function in the Euclidean region looks quite similar, there are essential differences which can be shown explicitly by calculating this Schwinger function. This means that this method is

indeed a useful way to determine whether the propagator corresponds to a confined particle or to a physical observable particle.

The difference in analytic structure is due to the difference in the infrared behavior of the photon, or more precisely, due to the different behavior of $\Pi(0)$ in the different approximations. In Fig. 7(b) we have plotted both the one-loop vacuum polarization, for massless and massive fermions, and the full vacuum polarization calculated numerically with dynamical massive fermions. Only in the infrared region there is a difference, and it is exactly this difference that causes the different behavior of the fermion propagator in the complex plane; it is also this infrared behavior which makes the potential confining or not. Therefore our conclusion is that (at least in this model) confinement is caused by the infrared behavior of the photon propagator, and is connected with complex mass-like singularities of the fermion propagator, thus preventing the fermions from being on mass-shell.

Finally, we should remark that these calculations are all done in the bare vertex approximation in the Landau gauge. It is known that the effects of vertex corrections, together with the wavefunction renormalization $Z(p)$ which we have set equal to 1, can change the results quite drastically [15,16,17]. Another question is what happens in other gauges, whether or not our results are gauge independent. As a qualitative indication whether or not our conclusions about confinement in QED3 also hold beyond the bare vertex approximation and in other gauges, we could compare our numerical vacuum polarization with the vacuum polarization as obtained by Burden *et al.* They solved the Dyson–Schwinger equation for the fermion propagator in quenched QED3 with the Ball–Chiu Ansatz for the vertex, and used this propagator to calculate the vacuum polarization, again with the Ball-Chiu vertex. Qualitatively our result for the vacuum polarization agrees with theirs, both in the infrared region, where we find a finite value of $\Pi(0)$ if we take into account the fermion mass, and in the ultraviolet region. In the infrared region there is a quantitative difference, but this can be explained by the fact that the value of $\Pi(0)$ strongly depends on the infrared value of the mass function $m(0)$, which is quite different in different approximations. Of course, we should keep in mind that if the behavior looks similar on the real axis, it does not necessarily mean that they are indeed similar in the entire complex plane. However, the fact that they also found a finite value of $\Pi(0)$ indicates that also beyond the bare vertex approximation there is a confining potential, and we would expect complex singularities as well. Whether or not these singularities are gauge independent (with a suitable vertex Ansatz), will be addressed in the future. Note that also the vacuum polarization itself should be explicitly gauge-independent.

VI. CONCLUSIONS

Our results show very clearly that there is a relation between a confining potential, the absence of stable asymptotic states, and complex mass-like singularities. Both in quenched QED3, and in massive QED3 using the $1/N$ expansion (with a dynamically generated fermion mass), there is a logarithmically confining potential, and we show that there are no stable asymptotic states. The Euclidean-time Schwinger function has an oscillatory behavior in these cases, indicating complex mass-like singularities. By solving the Dyson–Schwinger equation directly in the complex momentum plane, we show that there are indeed such complex singularities.

On the other hand, using massless bare fermions in the one-loop vacuum polarization, there is no confining potential. In this approximation, the Schwinger function indicates a stable asymptotic state. A direct analysis of the Dyson–Schwinger equation in the complex plane reveals that there are complex singularities even in this case, but that they are located very close to the real timelike axis. Given the approximations made, it is not unreasonable to assume that this small (less than 10%) deviation from the real timelike axis is caused by the truncation of the Dyson–Schwinger equation.

These results are obtained with a dynamically generated fermion mass, starting with massless bare fermions. For $N > N_c$, in the chirally symmetric phase, there is no dynamical fermion mass, and the fermion propagator has a singularity at the origin, just as the bare one. This also agrees with the fact that in there is no confining potential in this massless phase (in the $1/N$ expansion), due to the infrared softening of the photon propagator in the presence of massless fermions. Thus the chiral phase transition is a confining phase transition as well, at least in this model.

Interpreting the absence of a mass singularity on the real axis in the timelike region as confinement does not completely explain the phenomenon of complex mass-like singularities. If they are indeed a genuine property of the full theory, it leads automatically to confinement, but it has more consequences. One of the consequences is that the naive Wick rotation is not allowed, and one should take into account the contributions coming from the complex singularities in going from Euclidean to Minkowski metric (and back). Another problem is connected with questions of unitarity an causality; however, one should keep in mind that these are requirements for the S-matrix of physical processes, and not necessarily for the propagator of an unphysical (confined) particle.

Another question is whether or not these complex singularities have a physical interpretation. Naively, the real part (or the absolute value) could be interpreted as the "constituent" mass, and the imaginary part as some "hadronization length", in terms of QCD and quark confinement. Such an interpretation is analogous to the interpretation of the poles of instable particles in terms of mass and decay width. A crucial requirement for such an interpretation is that the singularities are gauge independent, which has to be studied in detail.

ACKNOWLEDGMENTS

I would like to thank Qing Wang, Craig Roberts, and David Atkinson for useful comments. This work has been financially supported by the Japanese Society for the Promotion of Science.

REFERENCES

* e-mail: maris@eken.phys.nagoya-u.ac.jp

[1] J.M. Cornwall, Phys. Rev. **D22**, 1452 (1980).
[2] V.Sh. Gogoghia and B.A. Magradze, Phys. Lett. **B217**, 162 (1989).
[3] V.N. Gribov, *Possible solution of the problem of quark confinement*, unpublished, U. of Lund preprint LU TP 91-7.
[4] C.D. Roberts, A.G. Williams, and G. Krein, Int. J. Mod. Phys. **A7**, 5607 (1992).
[5] for a review, see C.D. Roberts and A.G. Williams, Progr. Part. and Nucl. Phys. **33**, 477 (1994), and references therein.
[6] D. Atkinson and D.W.E. Blatt, Nucl. Phys. **B151**, 342 (1979).
[7] S.J. Stainsby and R.T. Cahill, Phys. Lett. **A146**, 467 (1990).
[8] P. Maris and H.A. Holties, Int. J. Mod. Phys. **A7**, 5369 (1992).
[9] S.J. Stainsby and R.T. Cahill, Int. J. Mod. Phys. **A7**, 7541 (1992).
[10] P. Maris, Phys. Rev. **D50**, 4189 (1994).
[11] C.J. Burden, J. Praschifka, and C.D. Roberts, Phys. Rev. **D46**, 2695 (1992).
[12] R.D. Pisarski, Phys. Rev. **D29**, 2423 (1984).
[13] T.W. Appelquist, M.J. Bowick, D. Karabali, and L.C.R. Wijewardhana, Phys. Rev. **D33**, 3704 and 3774 (1986); T.W. Appelquist, D. Nash, and L.C.R. Wijewardhana, Phys. Rev. Lett. **60**, 2575 (1988); D. Nash, Phys. Rev. Lett. **62**, 3024 (1989).
[14] E. Dagotto, A. Kocić, and J.B. Kogut, Phys. Rev. Lett. **62**, 1083 (1989); Nucl. Phys. **B334**, 279 (1990).
[15] M.R. Pennington and S.P. Webb, *Hierarchy of scales in three dimensional QED*, unpublished, Brookhaven Nat. Lab. preprint, BNL-40886 (1988).
[16] D. Atkinson, P.W. Johnson and P. Maris, Phys. Rev. **D42**, 602 (1990).
[17] M.R. Pennington and D. Walsh Phys. Lett. **B253**, 246 (1991); D.C. Curtis, M.R. Pennington, and D. Walsh Phys. Lett. **B295**, 313 (1992).
[18] C. Itzykon and J.-B. Zuber, *Quantum Field Theory* (McGraw-Hill, New York, 1980).
[19] see e.g. Chap. 6 of J. Glimm and A. Jaffe, *Quantum Physics* (Springer-Verlag, New Yrork, 1987).
[20] C. Vafa and E. Witten, Commun. Math. Phys. **95**, 257 (1984).
[21] R. Jackiw and S. Templeton, Phys.Rev. **D23**, 2291 (1981); T.W. Appelquist and R.D. Pisarski, Phys.Rev. **D23**, 2305 (1981); T.W. Appelquist and U. Heinz, Phys.Rev. **D23**, 2169 (1981).
[22] M. Göpfert and G. Mack, Commun. Math. Phys. **82**, 545 (1982).
[23] P. Maris, *Nonperturbative analysis of the fermion propagator: dynamical mass generation and complex singularities*, Ph.D. Thesis, U. of Groningen, 1993.
[24] L.C. Hollenberg, C.D. Roberts, and B.H.J. McKellar, Phys. Rev. **C46**, 2057 (1992).

FIGURES

FIG. 1. The analytic structure of a full, stable, physical observable particle, in (a) the p_0-plane and (b) the p^2-plane (in Minkowski metric).

FIG. 2. The analytic continuation into the complex momentum plane of the integral equation (in Euclidean momenta).

FIG. 3. The Schwinger function for quenched QED3 ($N = 0$, diamonds) and with the one-loop vacuum polarization ($N = 2$, plusses), (a) the logarithmic derivative, (b) the logarithm of its absolute value; the energy scale is defined by requiring $m(0) = 1$.

FIG. 4. The logarithm of the absolute value of the Schwinger function with $N = 2$ and some different approximations for the photon propagator: with the one-loop vacuum polarization of massless fermions (Eq. (12), plusses), with that of fermions with a fixed mass $m(0)$ (Eq. (13), crosses), and with the full vacuum polarization with dynamical fermions (squares); for comparison, we also included the quenched results (diamonds).

FIG. 5. The infrared mass $m(0)$ with the one-loop vacuum polarization of massless fermions (solid line) and with the full vacuum polarization (diamonds), as a function of N

FIG. 6. The phase ϕ of the mass-singularity obtained with the one-loop vacuum polarization of massless fermions (both the results of using the integral equation Eq. (34) directly, and that of using a differential equation which can be derived from it, after some further approximations, see [23]), and with the full vacuum polarization (diamonds), as a function of N; for completeness we have included the value for quenched QED3 at $N = 0$. The dotted line corresponds to $\phi = \pi/2$, which means a mass singularity on the real timelike axis.

FIG. 7. The mass function (a) and vacuum polarization (b) as obtained by taking into account the one-loop vacuum polarization of massless fermions (dotted line), that of fermions with a fixed mass $m(0)$ (dashed line), and that of dynamical fermions (solid line), all for $N = 2$ and in units of α; for completeness we included the mass function for quenched QED3 (dashed-dotted line) in (a).

TABLES

	Schwinger function		Direct search	
N	Re(μ)	Im(μ)	Re(μ)	Im(μ)
quenched QED3 (μ in units of e^2)				
0	0.082	0.073	0.0715	0.0760
massless fermions in the vacuum polarization (μ in units of α)				
1	0.13	0	0.128	2.88e-2
2	2.6e-3	0	2.67e-3	1.4e-4
3	1.8e-9	0	1.9e-9	7e-11
dynamical fermions in the vacuum polarization (μ in units of α)				
1	0.25	0.2	0.23	0.21
2	0.008	0.007	0.008	0.006

TABLE I. Estimates for the mass-singularities in the quenched approximation, with massless fermions in the vacuum polarization and with the full vacuum polarization, using both the Euclidean-time Schwinger function and a direct search in the complex momentum plane.

Figure 1

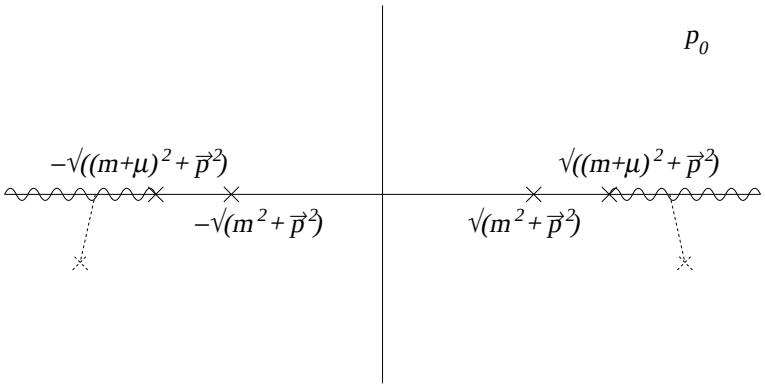
p_0
$-\sqrt{((m+\mu)^2+\vec{p}^2)}$
$\sqrt{((m+\mu)^2+\vec{p}^2)}$
$-\sqrt{(m^2+\vec{p}^2)}$
$\sqrt{(m^2+\vec{p}^2)}$

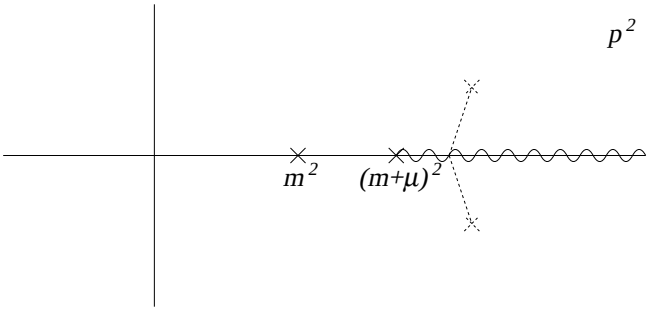
p^2
m^2
$(m+\mu)^2$

Figure 2

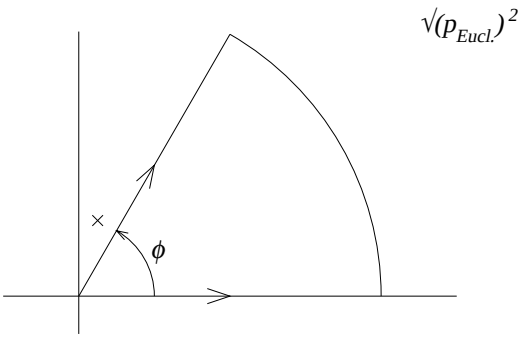

Figure 3a

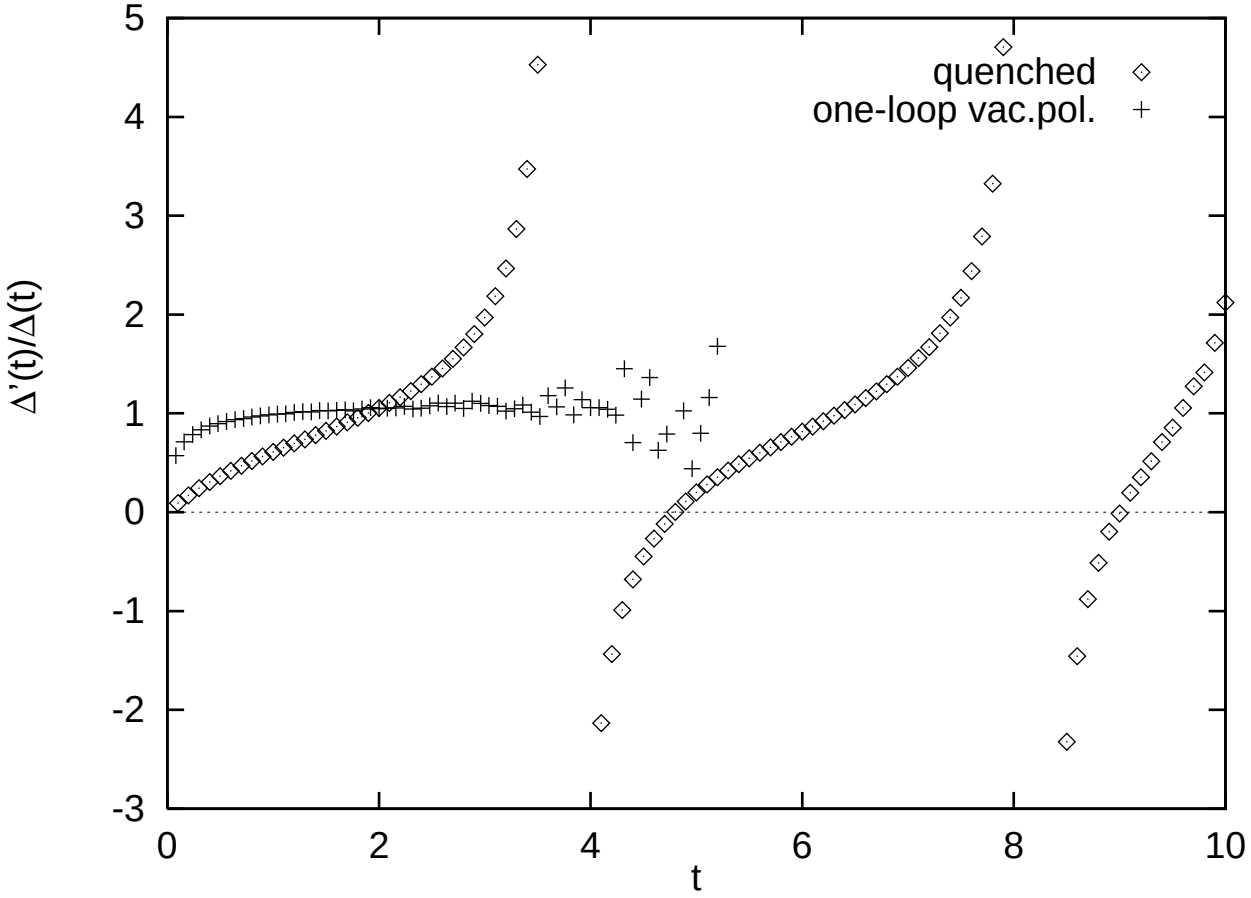

Figure 3b

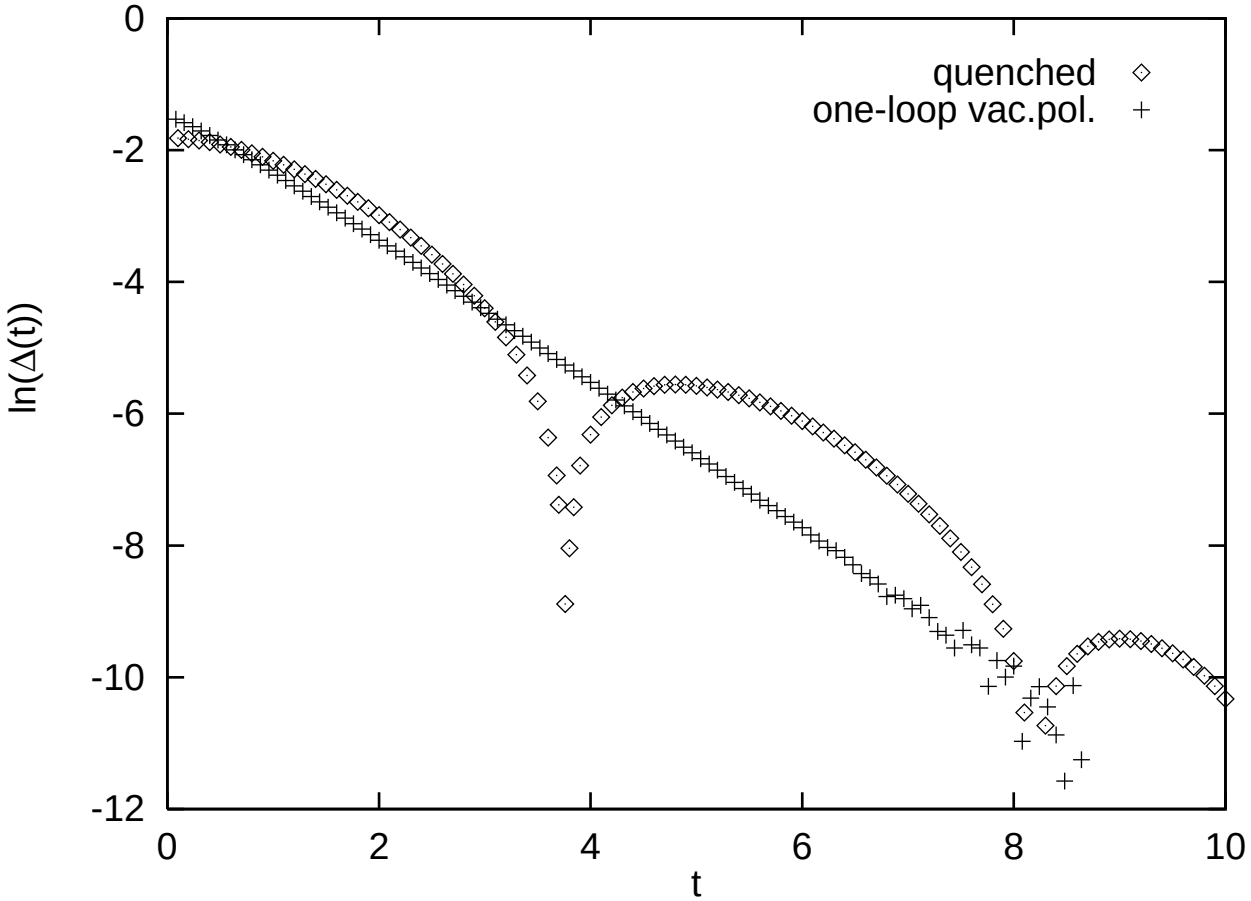

Figure 4

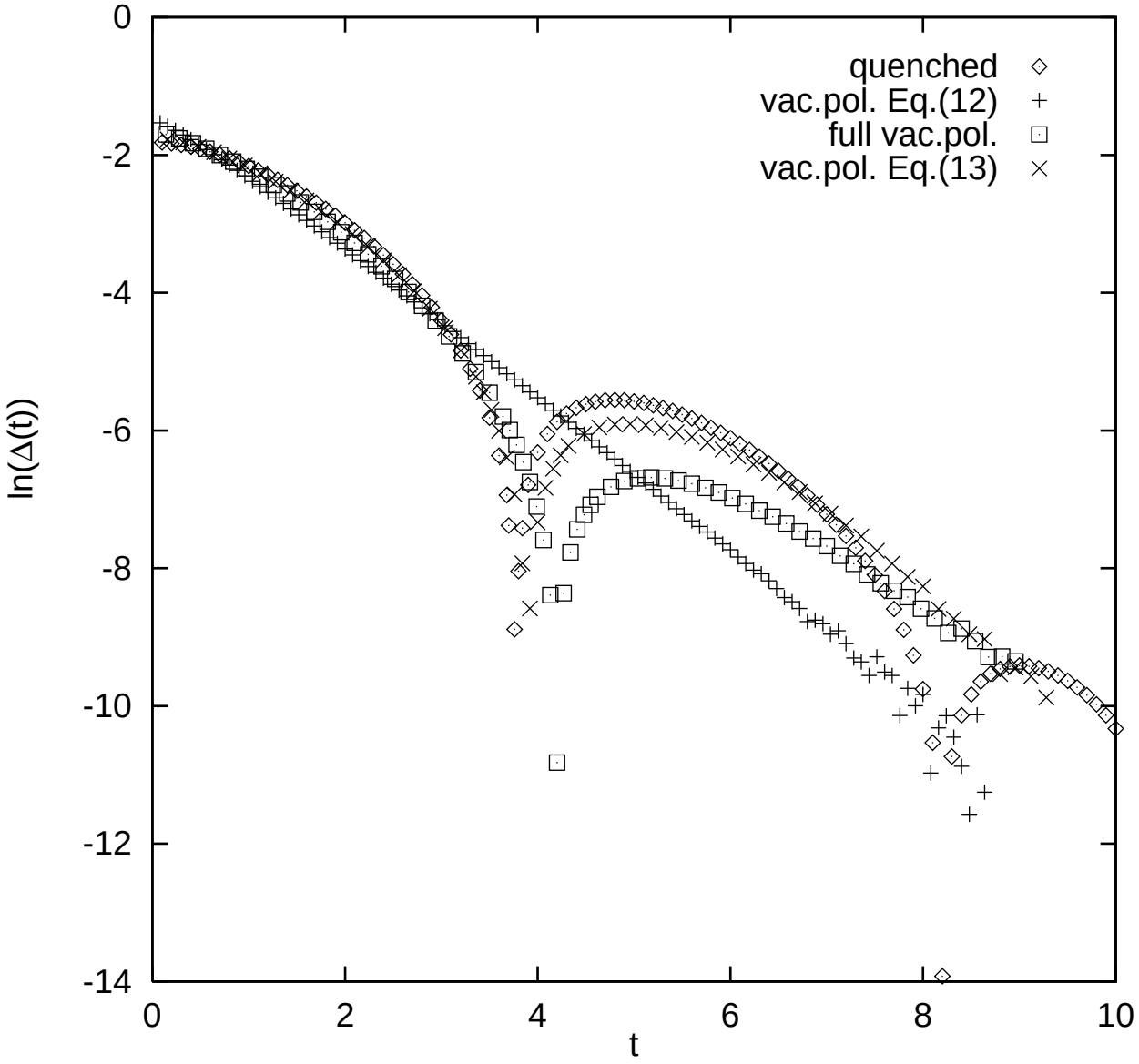
quenched
vac.pol. Eq.(12)
full vac.pol.
vac.pol. Eq.(13)
ln(Δ(t))
t
0
-2
-4
-6
-8
-10
-12
-14
0
2
4
6
8
10

Figure 5

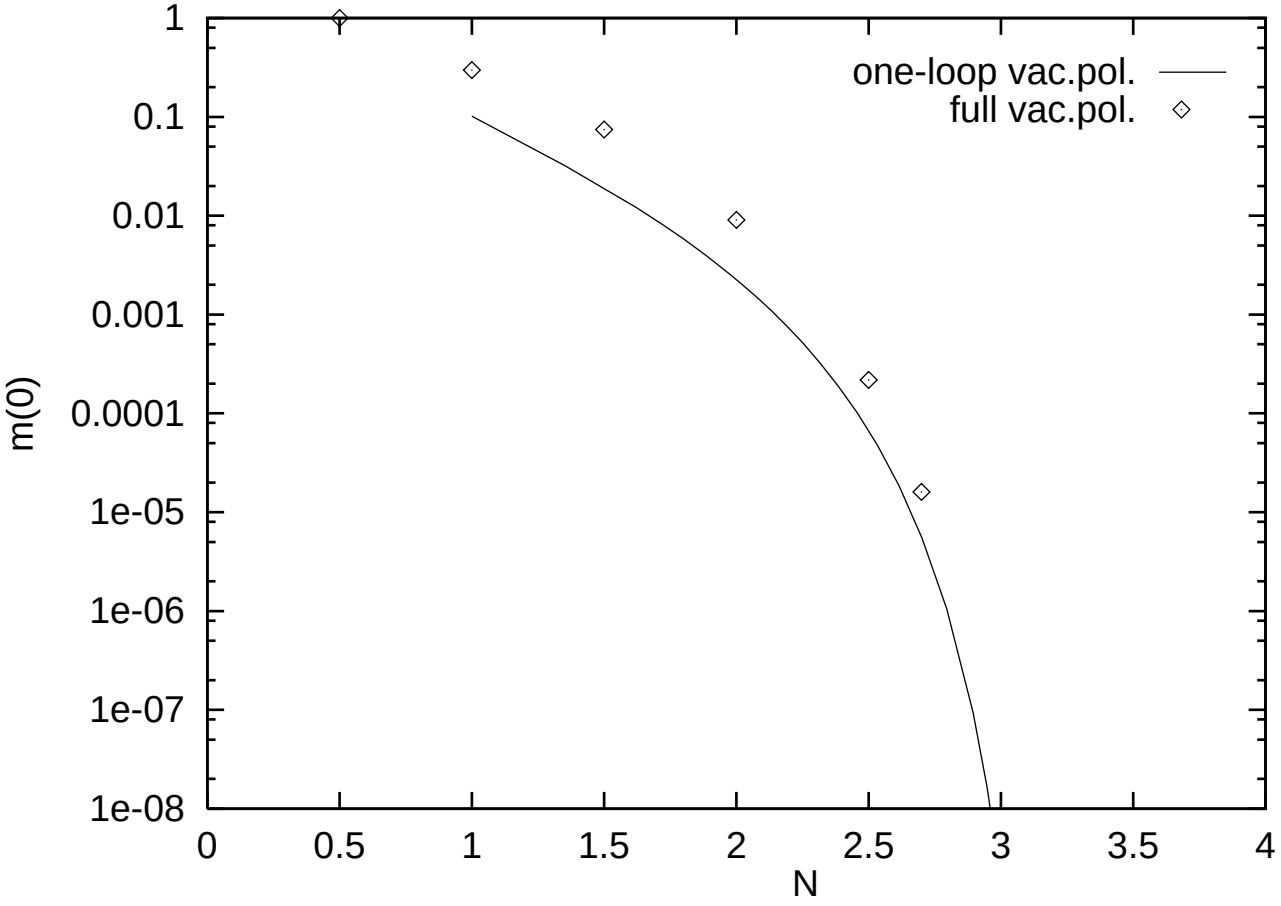
one-loop vac.pol.
full vac.pol.
m(0)
N
1
0.1
0.01
0.001
0.0001
1e-05
1e-06
1e-07
1e-08
0
0.5
1
1.5
2
2.5
3
3.5
4

Figure 6

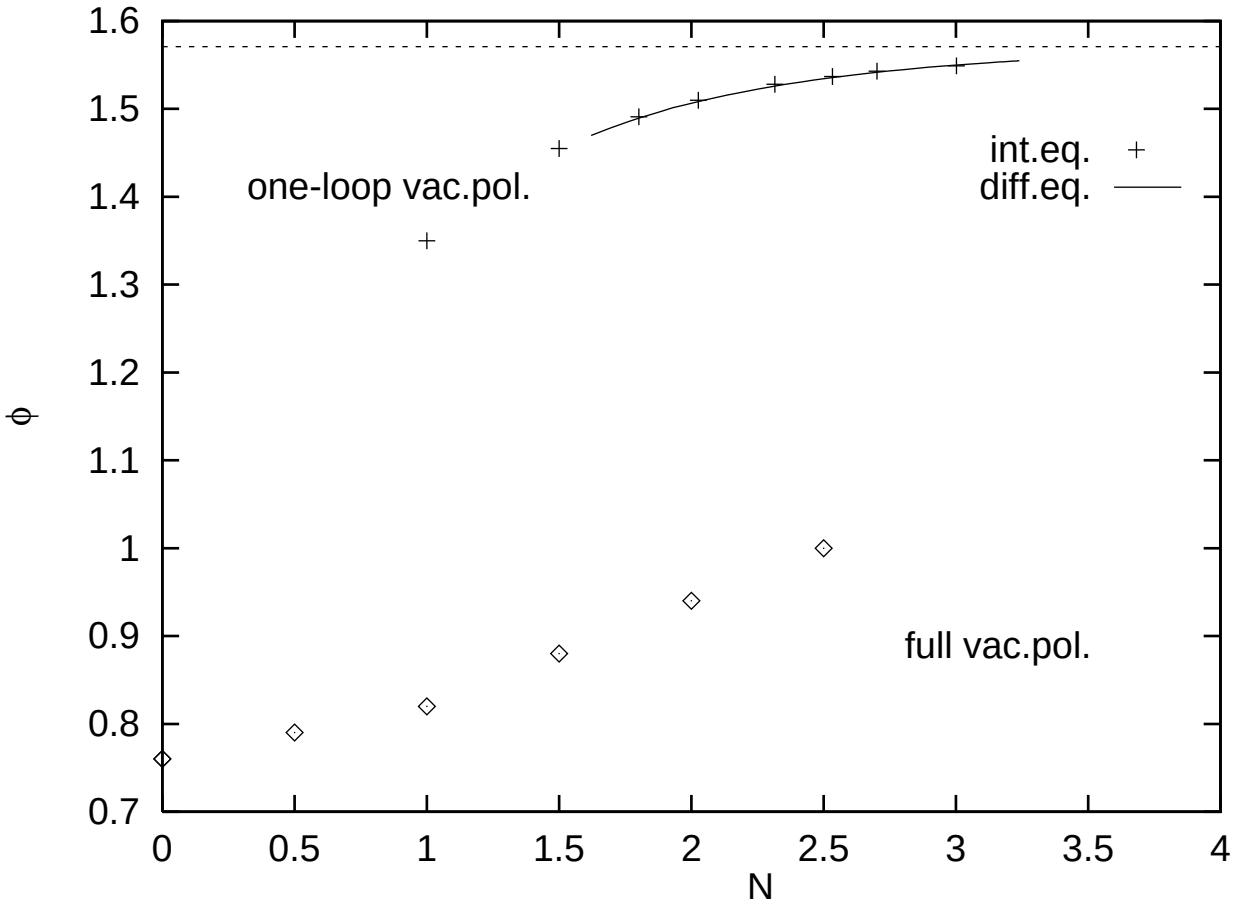
1.6
1.5
1.4
1.3
1.2
1.1
1
0.9
0.8
0.7
φ
0
0.5
1
1.5
2
2.5
3
3.5
4
N
int.eq.
diff.eq.
one-loop vac.pol.
full vac.pol.

Figure 7a

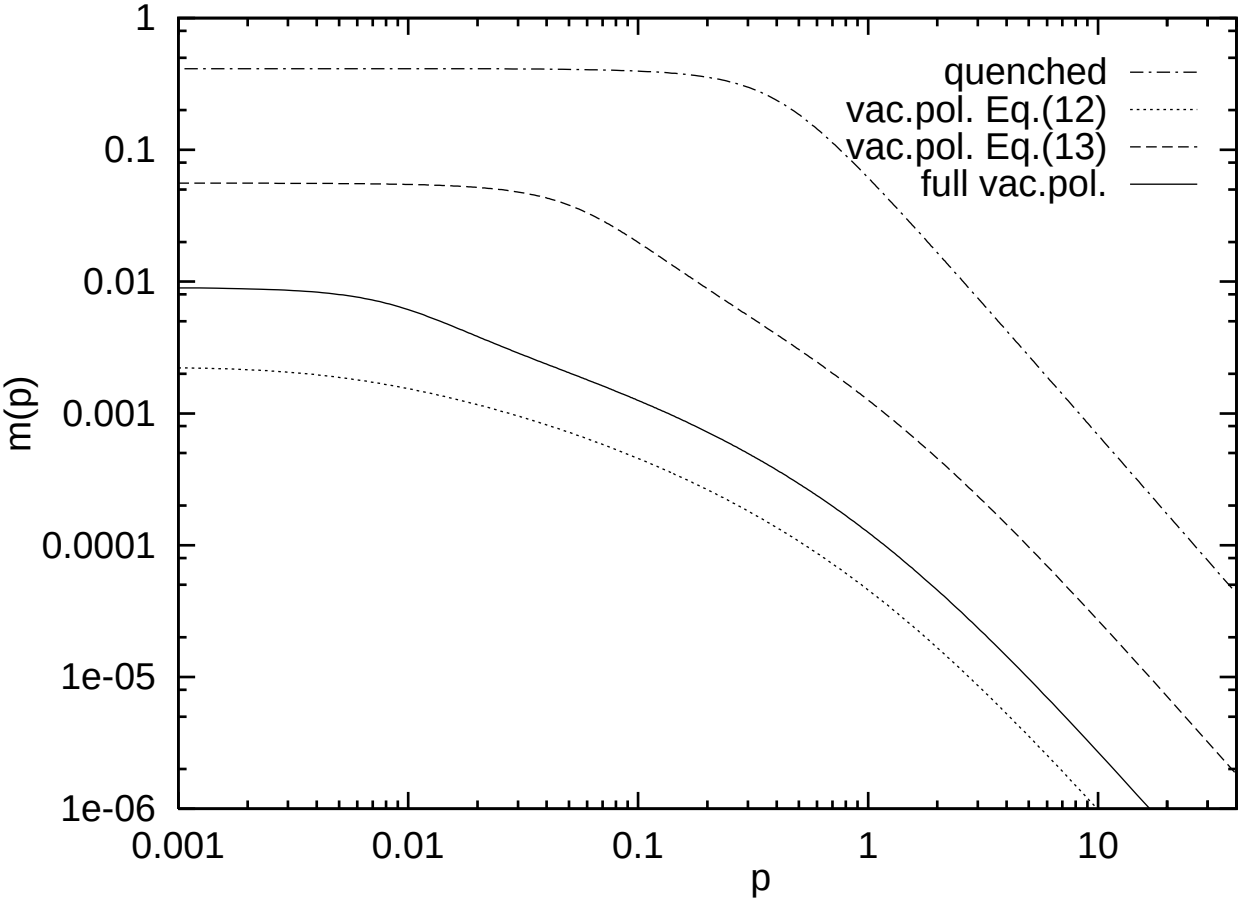

Figure 7b